Jurnal Teknologi

Full Paper

CHARACTERIZATION OF REDUCED GRAPHENE OXIDE/ACTIVATED CARBON-BASED ELECTRODE CONTAINING MIXING CMC-SBR BINDER AND APPLICATION IN SUPERCAPACITOR

Mohd Asyadi Azam[a*], M. F. Aziz[a,b], T. A. T. Adaham[a], N. E. Safie[a], M. Mupit[c], Akito Takasaki[d]

[a]Fakulti Kejuruteraan Pembuatan, Universiti Teknikal Malaysia Melaka, Hang Tuah Jaya, 76100 Durian Tunggal, Melaka, Malaysia
[b]School of Physics, Universiti Sains Malaysia, 11800 USM, Penang, Malaysia
[c]Faculty of Chemical Engineering, Universiti Kuala Lumpur, Kawasan Perindustrian Taboh Naning, 78000 Alor Gajah, Melaka, Malaysia
[d]Department of Engineering Science and Mechanics, Shibaura Institute of Technology, 3-7-5 Toyosu, Koto-ku, Tokyo, 135-8548, Japan

Article history
Received
16 November 2021
Received in revised form
15 June 2022
Accepted
25 July 2022
Published Online
31 October 2022

*Corresponding author
asyadi@utem.edu.my

Graphical abstract

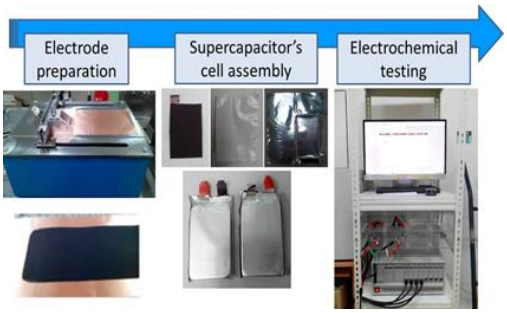

Abstract

In this work, variation of mixing a combination of carboxymethylcellulose (CMC) and styrene-butadiene rubber (SBR) as both used as the binder in the electrode has been studied. The purpose of using CMC-SBR as the binder in the electrode is to achieve a high supercapacitor performance. The electrode preparation has been carried out by mixing the reduced graphene oxide (rGO) and activated carbon (AC) in a blender. The binder preparation started by dissolving the CMC and SBR in the deionized water using a clean glass container. Then, rGO/AC has been stirred with the CMC-SBR for 60 minutes until a homogenous slurry formed. All electrodes have been characterized with Raman spectroscopy. The electrochemical tests such as cyclic voltammetry (CV) and galvanostatic charge-discharge (GCD) for all electrode compositions were performed. The electrode with 4:6 (in weight percentage) of CMC-SBR shows the highest specific capacitance (C_{sp}) of 59.65 F g^{-1} (CV scan rate of 1 mV s^{-1}) and 12.82 F g^{-1} from GCD test. This confirmed that the electrode containing 4 wt.% of CMC and 6 wt.% of SBR resulting in the best composition, which is reliable and practical for the supercapacitor application.

Keywords: rGO/AC, supercapacitor electrode, CMC-SBR binder, cyclic voltammetry, charge-discharge

Abstrak

Dalam projek ini, variasi pencampuran gabungan karboksimetilselulosa (CMC) dan getah stirena-butadiena (SBR) kerana kedua-duanya digunakan sebagai pengikat dalam elektrod telah dikaji. Penyediaan elektrod telah dijalankan dengan mencampurkan graphene oxide (rGO) dan karbon teraktif (AC) di dalam pengisar. Penyediaan pengikat dimulakan dengan melarutkan CMC dan SBR dalam air ternyahion menggunakan bekas kaca

bersih. Kemudian, rGO/AC telah dikacau dengan CMC-SBR selama 60 minit sehingga buburan homogen terbentuk. Semua elektrod telah dicirikan dengan spektroskopi Raman. Ujian elektrokimia seperti voltammetri kitaran (CV) dan nyahcas cas-galvanostatik (GCD) untuk semua komposisi elektrod telah dilakukan. Elektrod dengan 4:6 (dalam peratusan berat) CMC-SBR menunjukkan kemuatan spesifik (Csp) tertinggi iaitu 59.65 F g^{-1} (kadar imbasan CV 1 mV s^{-1}) dan 12.82 F g^{-1} daripada ujian GCD. Ini mengesahkan bahawa elektrod yang mengandungi 4 wt.% CMC dan 6 wt.% SBR menghasilkan komposisi terbaik, yang boleh dipercayai dan praktikal untuk aplikasi superkapasitor.

Kata kunci: rGO/AC, elektrod superkapasitor, pengikat CMC-SBR, voltammetri kitaran, superkapasitor

1.0 INTRODUCTION

Supercapacitor with low specific capacitance (C_{sp}) is one of the crucial problems in the energy storage field [1-5]. In exploring the best combination of elements (active material, binder, and solvent) in the electrode for the supercapacitor fabrication, some criteria need to approach giving a high specific capacitance value in the supercapacitor [6-10].

The previous study used polyvinylidene difluoride (PVDF) and polytetrafluoroethylene (PTFE) as a binder in the electrodes. However, both binders are unsuitable for future research due to the high pricing, fluorine pollution, and toxicity [11]. A dual binder carboxymethylcellulose (CMC) and styrene-butadiene rubber (SBR) has been used due to several advantages such as good adhesion to the current collector, water-based solubility, and enabling aqueous processing [11]. In this study, the different CMC and SBR which used as the binder materials in the reduced graphene oxide/ activated carbon (rGO/AC) supercapacitor electrode has been studied. Notably, the elastomeric binder has been produced by combining the strong CMC with SBR thickening agent for the rGO/AC electrode preparation [11,12].

This study aims to produce the best composition amount of CMC-SBR binder in the electrode for achieving a high-performance supercapacitor.

2.0 METHODOLOGY

As per Figure 1, the electrode preparation has been carried out by mixing the reduced graphene oxide (rGO) and activated carbon (AC) in a mixing blender. At the same time, the binder preparation has been started by dissolving the carboxymethylcellulose (CMC) and styrene-butadiene rubber (SBR) in the deionized water using a clean glass container. The CMC-SBR compositions were varied to 2:8, 3:7, 4:6, and 5:5 in wt. % which referred from previous research [11]. rGO/AC has been stirred in the CMC-SBR binder for 60 minutes until a homogenous slurry has produced. Then, the slurry was coated on a clean copper foil using the applicator. The coated copper foil was then placed in a drying oven for 12 hours at a constant temperature of 100 °C and stored in a closed desiccator with a low humidity environment.

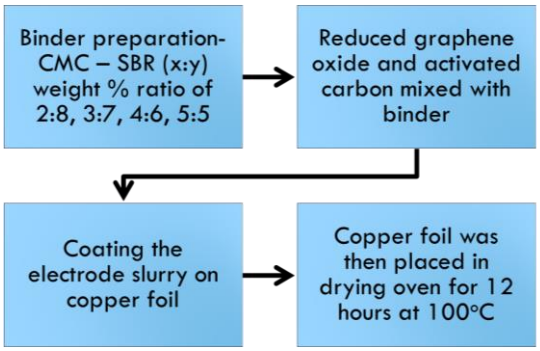

Figure 1 Schematic diagram for the electrode preparation

All prepared electrodes have been characterized with Raman spectroscopy. The samples for 2 wt. % CMC – 8 wt. % SBR, 3 wt. % CMC – 7 wt. % SBR, 4 wt. % CMC – 6 wt. % SBR, and 5 wt. % CMC – 5 wt. % SBR were designated for electrode A, B, C, and D, respectively (Table 1).

For the supercapacitor assembly, the electrode has been punched out at constant size (15 mm) and configured in a supercapacitor jig. In the jig, the polypropylene (PP) separator was sandwiched together by the two symmetric electrodes cell in the stainless steels compartment. The potassium hydroxide (6M KOH) electrolyte has been used as electrolyte in this supercapacitor which later being used for the electrochemical tests such as cyclic voltammetry (CV) and galvanostatic charge-discharge (GCD).

Table 1 Composition for all electrodes

Sample	CMC-SBR weight ratio	CMC (g)	SBR (g)	rGO (g)	AC (g)
A	2:8	0.4	1.6	8.0	10.0
B	3:7	0.6	1.4	8.0	10.0
C	4:6	0.8	1.2	8.0	10.0
D	5:5	1.0	1.0	8.0	10.0

3.0 RESULTS AND DISCUSSION

In Figure 2, Raman spectra for all the electrode A, B, C, and D has been shown properly. From this Raman pattern, the ratio intensity of D-band (I_D) and G-band (I_G) can be calculated using this formula:

$$\text{Intensity ratio} = I_D/I_G \quad (1)$$

From Table 2, I_D/I_G is increasing from electrode A to electrode C (0.968 to 1.003) showing that the amorphous carbon is dominating in the electrode. This phenomenon is because the D band, related to the disordered carbon structure or amorphous carbon, is more dominant in the electrode than the G band, which is related to the graphitic structure or carbon whiskers. The higher amorphous region should improve the ions (from the electrolyte) mobile in the electrode-electrolyte surface [13].

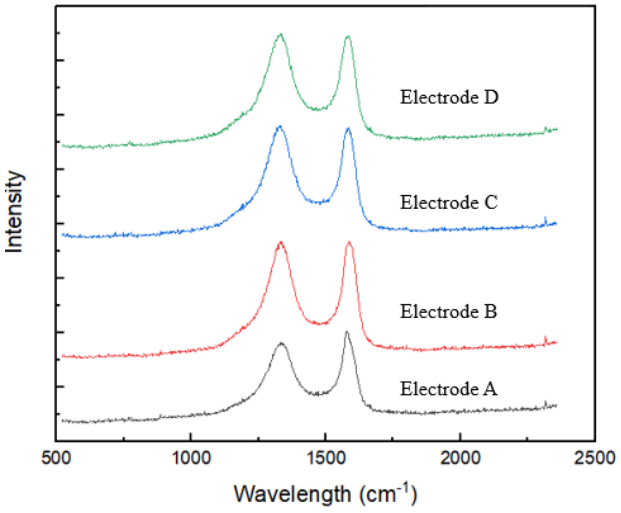

Figure 2 Raman pattern for electrode A, B, C, and D

Table 2 I_D/I_G intensity ratio for all electrodes

	A (cm^{-1})	B (cm^{-1})	C (cm^{-1})	D (cm^{-1})
Band D	1334.70	1334.70	1334.70	1332.42
Band G	1577.52	1586.64	1586.64	1584.36
I_D/I_G	**0.968**	**1.002**	**1.003**	**1.000**

From Figure 3, the cyclic voltammetry curves at different scan rate (1, 5, 10, 30, 50, 70, 100, and 150 mV s^{-1}) for electrode C (4 wt. % CMC – 6 wt. % SBR) has been shown nicely. The specific capacitance, C_{sp} has been obtained for all electrodes prepared, resulting electrode C has the highest C_{sp} of 59.65 Fg^{-1} at 1 mV s^{-1} (as refer in the Table 3). The decreasing specific capacitance, C_{sp}, with the increasing scan rate is due to the ion concentration (from the electrolyte) on the layer between electrode and electrolyte suddenly improving. The electrochemical activity also has been interrupted due to the lack of ion diffusion from the electrolyte-electrode surface [14-16]. This C_{sp} value are comparable with other work [14-17].

Table 3 Specific capacitance, C_{sp} for electrode C (4 wt. % CMC – 6 wt. % SBR) sample

Scan rate, mVs^{-1}	C_{sp} ($F\ g^{-1}$)
1	59.65
5	20.54
10	12.12
30	4.97
50	3.34
70	2.32
100	1.63
150	1.08

From Figure 4, the GCD curve at different scan rates starts from 0.3, 0.5, and 0.7 Ag^{-1} has properly shown. The variation of these scan rates has followed from previous research [18]. From the CD curve, the specific capacitance (C_{sp}) for each scan rate has been obtained, which is the highest value of C_{sp} (12.82 Fg^{-1}) has shown at a scan rate of 0.3 Ag^{-1} (Table 4). This phenomenon suggests this electrode composition retains a good supercapacitor performance [18-20]. However, the difference in obtained C_{sp} from the CV and GCD is because of the uneven electrode preparation and electrode-electrolyte assembly [18].

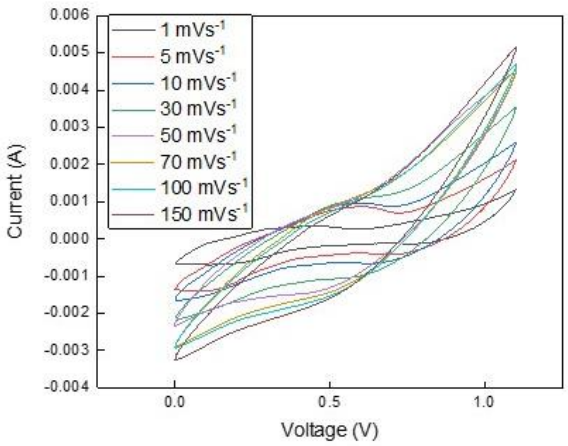

Figure 3 CV curves at different scan rates (1, 5, 10, 30, 50, 70, 100, 150 mVs^{-1}) for sample electrode C (4 wt. % CMC – 6 wt. % SBR)

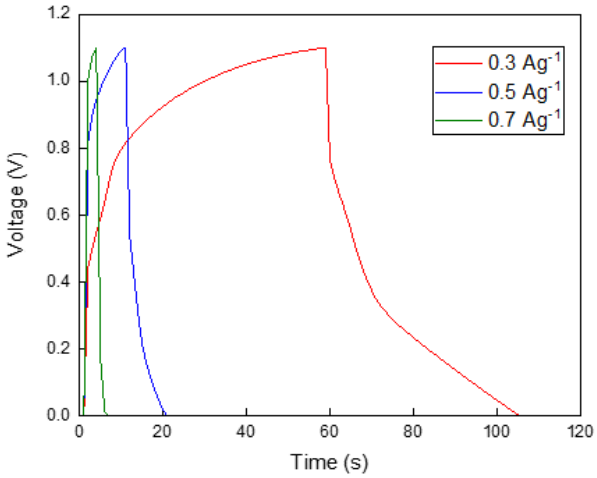

Figure 4 GCD curves at different current density (0.3, 0.5, and 0.7 Ag^{-1}) for electrode C (4 wt. % CMC -6 wt. % SBR)

Table 4 C_{sp} for each current density (electrode C)

Current density (Ag^{-1})	C_{sp} (Fg^{-1})
0.3	12.82
0.5	5.24
0.7	1.71

4.0 CONCLUSION

All electrodes with varied amounts of CMC-SBR have been produced. I_D/I_G for electrode C has the highest value of 1.003 confirming that the amorphous carbon is dominating in the electrode. In the CV test, the electrode C (4 wt. % CMC – 6 wt. % SBR) attained the highest specific capacitance of 59.65 Fg^{-1} (scan rate of 1 mVs^{-1}). The GCD curve of electrode C obtains equally with an ideal supercapacitor symmetric triangle shape. It can be determined that electrode C has the best composition for high-performance supercapacitor assembly. This evaluation has opened a potential development of new kind of binder material for high performance energy storage device.

Acknowledgement

Authors would like to acknowledge Universiti Teknikal Malaysia Melaka and Ministry of Higher Education (MOHE) Malaysia for the research grant numbered PRGS/2018/FKP-AMC/T00019 as well as the facilities support.

References

[1] Sajjad, M. and Lu, W., 2021. Covalent Organic Frameworks Based Nanomaterials: Design, Synthesis, and Current Status for Supercapacitor Applications: A Review. *Journal of Energy Storage*. 39: 102618. DOI: https://doi.org/10.1016/j.est.2021.102618.

[2] Zha, X., Wu, Z., Cheng, Z., Yang, W., Li, J., Chen, Y., He, L., Zhou, E. and Yang, Y., 2021. High Performance Energy Storage Electrodes Based on 3D Z-CoO/RGO Nanostructures for Supercapacitor Applications. *Energy*. 220: 119696. DOI: https://doi.org/10.1016/j.energy.2020.119696.

[3] Azam, M. A., Ramli, N. S. N., Nor, N. A. N. M. and Nawi, T. I. T. 2021. Recent Advances in Biomass-derived Carbon, Mesoporous Materials, and Transition Metal Nitrides as New Electrode Materials for Supercapacitor: A Short Review. *International Journal of Energy Research*. 45(6): 8335-8346. DOI: https://doi.org/10.1002/er.6377.

[4] Mehra, P., Singh, C., Cherian, I., Giri, A. and Paul, A. 2021. Deciphering the Incredible Supercapacitor Performance of Conducting Biordered Ultramicroporous Graphitic Carbon. *ACS Applied Energy Materials*. 4(5): 4416-4427. DOI: https://doi.org/10.1021/acsaem.1c00020.

[5] Abbasi, L., Arvand, M. and Moosavifard, S. E. 2020. Facile Template-Free Synthesis of 3D Hierarchical Ravine-like Interconnected MnCo2S4 Nanosheet Arrays for Hybrid Energy Storage Device. *Carbon*. 161: 299-308. DOI: https://doi.org/10.1016/j.carbon.2020.01.094.

[6] Rui, B., Yang, M., Zhang, L., Jia, Y., Shi, Y., Histed, R., Liao, Y., Xie, J., Lei, F. and Fan, L. 2020. Reduced Graphene Oxide-Modified Biochar Electrodes via Electrophoretic Deposition with High-Rate Capability for Supercapacitors. *Journal of Applied Electrochemistry*. 50(4): 407-420. DOI: https://doi.org/10.1007/s10800-020-01397-1.

[7] Purkait, T., Singh, G., Kumar, D., Singh, M. and Dey, R. S. 2018. High-Performance Flexible Supercapacitors Based on Electrochemically Tailored Three-Dimensional Reduced Graphene Oxide Networks. *Scientific Reports*. 8(1): 1-13. DOI: https://doi.org/10.1038/s41598-017-18593-3.

[8] Wang, C., Zhou, J. and Du, F. 2016. Synthesis of Highly Reduced Graphene Oxide for Supercapacitor. *Journal of Nanomaterials*. DOI: https://doi.org/10.1155/2016/4840301.

[9] Mishra, R. K., Choi, G. J., Sohn, Y., Lee, S. H. and Gwag, J. S. 2020. A Novel RGO/N-RGO Supercapacitor Architecture for A Wide Voltage Window, High Energy Density and Long-life via Voltage Holding Tests. *Chemical Communications*. 56(19): 2893-2896. DOI: https://doi.org/10.1039/D0CC00249F.

[10] Govindarajan, D., Uma Shankar, V. and Gopalakrishnan, R. 2019. Supercapacitor Behavior and Characterization of RGO Anchored V2O5 Nanorods. *Journal of Materials Science: Materials in Electronics*. 30(17): 16142-16155. DOI: https://doi.org/10.1007/s10854-019-01984-9.

[11] Cheng, Y., Ren, X., Duan, L. and Gao, G. 2020. A Transparent and Adhesive Carboxymethyl Cellulose/Polypyrrole Hydrogel Electrode for Flexible Supercapacitors. *Journal of Materials Chemistry C*. 8(24): 8234-8242. DOI: https://doi.org/10.1039/D0TC01039A.

[12] Kumagai, S., Mukaiyachi, K. and Tashima, D. 2015. Rate and Cycle Performances of Supercapacitors with Different Electrode Thickness Using Non-Aqueous Electrolyte. *Journal of Energy Storag*. 3: 10-17. DOI: https://doi.org/10.1016/j.est.2015.08.002.

[13] Chang, S., Zhang, Y., Zhang, B., Cao, X., Zhang, L., Huang, X., Lu, W., Ong, C.Y.A., Yuan, S., Li, C. and Huang, Y. 2021. Conductivity Modulation of 3D-Printed Shellular Electrodes Through Embedding Nanocrystalline Intermetallics into Amorphous Matrix for Ultrahigh-Current Oxygen Evolution. *Advanced Energy Materials*. 11(28): 2100968. DOI: https://doi.org/10.1002/aenm.202100968.

[14] Maharsi, R., Arif, A. F., Ogi, T., Widiyandari, H. and Iskandar, F. 2019. Electrochemical Properties of TiO x/rGO Composite as an Electrode for Supercapacitors. *RSC Advances*. 9(48): 27896-27903. DOI: https://doi.org/10.1039/C9RA04346B.

[15] Siva, V., Murugan, A., Shameem, A., Thangarasu, S. and Bahadur, S. A. 2022. A Facile Microwave-Assisted Combustion Synthesis of NiCoFe2O4 Anchored Polymer Nanocomposites as an Efficient Electrode Material for

Asymmetric Supercapacitor Application. *Journal of Energy Storage*. 48: 103965.
DOI: https://doi.org/10.1016/j.est.2022.103965.

[16] Karamanova, B., Stoyanova, A., Shipochka, M., Girginov, C. and Stoyanova, R. 2019. On The Cycling Stability of Biomass-derived Carbons as Electrodes in Supercapacitors. *Journal of Alloys and Compounds*. 803: 882-890.
DOI: https://doi.org/10.1016/j.jallcom.2019.06.334.

[17] Parashtekar, A., Bourgeois, L. and Tatiparti, S. S. V. 2022. Stoichiometry–Grain Size-Specific Capacitance Interrelationships in Nickel Oxide. *RSC Advances*. 12(14): 8333-8344.
DOI: https://doi.org/10.1039/D1RA09000C.

[18] Abid, M. A. A. M., Radzi, M. I., Mupit, M., Osman, H., Munawar, R. F., Samat, K. F., Suan, M. S. M., Isomura, K. and Islam, M. R. 2020. Cyclic Voltammetry and Galvanostatic Charge-Discharge Analyses of Polyaniline/Graphene Oxide Nanocomposite Based Supercapacitor. *Malaysian Journal on Composites Science & Manufacturing*. 3(1): 14-26.
DOI: https://doi.org/10.37934/mjcsm.3.1.1426.

[19] Huang, M., Wang, L., Chen, S., Kang, L., Lei, Z., Shi, F., Xu, H. and Liu, Z. H. 2017. Highly Flexible All-Solid-State Cable-Type Supercapacitors Based on Cu/Reduced Graphene Oxide/Manganese Dioxide Fibers. *Rsc Advances*. 7(17): 10092-10099.
DOI: https://doi.org/10.1039/C6RA28117F.

[20] Seman, R. N. A. R., Azam, M. A. and Ani, M. H. 2018. Graphene/Transition Metal Dichalcogenides Hybrid Supercapacitor Electrode: Status, Challenges, and Perspectives. *Nanotechnology*. 29(50): 502001.
DOI: https://doi.org/10.1088/1361-6528/aae3da.